Received: 21 December 2021 | Accepted: 16 August 2022

DOI: 10.1111/1752-1688.13068

AMERICAN WATER RESOURCES ASSOCIATION JAWRA JOURNAL OF THE AMERICAN WATER RESOURCES ASSOCIATION

RESEARCH ARTICLE

Pre-instrumental perspectives on Arkansas River cross-watershed flow variability

Max C. A. Torbenson[1] | David W. Stahle[2] | Ian M. Howard[2] | Joshua M. Blackstock[2] | Malcolm K. Cleaveland[2] | James H. Stagge[1]

[1]Department of Civil, Environmental and Geodetic Engineering, The Ohio State University, Columbus, Ohio, USA

[2]Department of Geosciences, University of Arkansas, Fayetteville, Arkansas, USA

Correspondence
Max C. A. Torbenson, Department of Civil, Environmental and Geodetic Engineering, The Ohio State University, Columbus, OH, USA.
Email: mtorbens@uni-mainz.de

Funding information
National Science Foundation, Grant/Award Number: 17-582

Abstract

We present four reconstruction estimates of Arkansas River baseflow and streamflow using a total of 78 tree-ring chronologies for three streamflow gages, geographically spanning the headwaters in Colorado to near the confluence of the Arkansas-Mississippi rivers. The estimates represent different seasonal windows, which are dictated by the shared limiting forcing of precipitation on seasonal tree growth and soil moisture—and subsequently on the variability of Arkansas River discharge. Flow extremes that were higher and lower than what has been observed in the instrumental era are recorded in each of the four reconstructions. Years of concurrent, cross-basin (all sites) low flow appear more frequently during the 20th and 21st Centuries compared to any period since 1600 A.D., however, no significant trend in cross-basin low flow is observed. As the most downstream major tributary of the Mississippi River, the Arkansas River directly influences flood risk in the Lower Mississippi River Valley. Estimates of extreme high flow in downstream reconstructions coincide with specific years of historic flooding documented in New Orleans, Louisiana, just upstream of the Mississippi River Delta. By deduction, Mississippi River flooding in years of low Arkansas River flow imply exceptional flooding contributions from the Upper Mississippi River catchments.

KEYWORDS
paleoclimatology, tree rings, flow separation, extremes

1 | INTRODUCTION

The Arkansas River is a major hydrological feature of the central United States (U.S.), from its headwaters in Colorado to the confluence of the Arkansas and Mississippi Rivers. Freshwater is scarce for most of the basin, as evident by extensive and unsustainable groundwater withdrawals in the region (Marston et al., 2015), and disputes over water rights (Naeser & Bennett, 1998). Reduced flows in the Great Plains sector of the Arkansas River have been measured since the mid-20th Century, partly due to surface and groundwater withdrawals for irrigation (Ferrington, 1993) and the impact of damming (Costigan & Daniels, 2012). These changes in the water budget have caused the river to become intermittent in Kansas and Oklahoma, with significant damage to the local ecosystems (e.g., Dodds et al., 2004). As a result, the Arkansas River exists as two separate surface streams at times, upstream and downstream of this extended central region of negligible flow.

Paper No. JAWR-21-0189-P of the *Journal of the American Water Resources Association* (JAWR).

Discussions are open until six months from issue publication.

Research impact statement

Tree ring-based reconstructions indicate that the Arkansas River has experienced high and low flows outside the range of observed extremes in the past four centuries.

The main drivers of inter-annual variability for Arkansas River streamflow are local and regional precipitation (Qiao et al., 2017). The water flowing in the river has the same source as the water being used for agriculture, and drought is a significant part of the climate-society interactions across the watershed. Although the river is not used extensively as a freshwater source in the east, it plays an important role for navigation and commerce. Extreme low and high flows can disrupt navigation (USACE, 2006) and it has been estimated that a 2-week disruption of business at Port of Catoosa, Oklahoma, could cause economic losses of over $180 million (Pant et al., 2015).

Flooding around the Arkansas River is also a reoccurring problem. In 2019, Oklahoma experienced significant damages after historic flooding and levee breaches in the month of May (Lewis & Trevisan, 2019). Flood levels were reached or exceeded on the lower Arkansas basin for 11 consecutive years between 1941 and 1951. The Arkansas River also contributes significant amounts of water as a tributary to the Mississippi River. Many of 20th and 21st Century New Orleans floods coincided with flooding and high flows of the Arkansas River, including the Great Flood of 1927 and the costly inundation in 1973 (Belt, 1975).

Streamflow has been measured in the upper basin at Cañon City, Colorado, since the 1890s, but instrumental records do not begin in the lower reaches of the basin until the late 1920s. These relatively short instrumental records, in combination with human interference through construction on and along the river (Horowitz, 2010; Keown et al., 1986), limit our understanding of the long-term (multi-decadal or centennial scale) natural variability of Arkansas River flow in terms of both the magnitude of extreme streamflow and low flow periods. While historical accounts of hydroclimatic variability exist (e.g., Mock, 1991), many do not document the full range of conditions that have been, and could feasibly be, experienced in the future.

Paleoclimatic reconstructions can provide longer perspectives. Tree rings have been used to extend the instrumental record of flow in many basins across the U.S., including the Colorado (e.g., Meko et al., 2007), the Missouri (Ravindranath et al., 2019), the Potomac (Maxwell et al., 2017), and the Delaware (Devineni et al., 2013) rivers, using methods of varying complexities. For western Arkansas River sites, proxy records in the form of soils (England et al., 2010) and tree rings (Woodhouse et al., 2011) have been used to study the frequency of flood and drought. These estimates aid in understanding long-term streamflow changes not only in the upper basin but have important implications for water resources several hundred miles downstream. Despite several paleoclimatic studies in the eastern part of the basin (e.g., Cleaveland, 2000; Cleaveland & Stahle, 1989; Torbenson & Stahle, 2018), there have been no attempts to reconstruct downstream Arkansas River flows.

In this paper, we present estimates of past Arkansas River flow at three gaging stations: near the headwaters in the Rocky Mountains, within the Great Plains in the central U.S., and above the confluence with the Mississippi River in the southeastern U.S. Four reconstructions are produced for various seasonal windows representing the relationship between flow and tree growth variability expressed as the respective correlations between local and extra-local precipitation. All reconstruction targets are important windows of the hydrological cycle of the Arkansas River, at their respective locations, and for the river basin as a whole. The reconstructions are validated against hold-out instrumental data outside the calibration period, as well as against historical accounts of extreme hydroclimatic events. The relative contribution of the Arkansas River to flooding in the Lower Mississippi River Valley (LMRV) is also analyzed through these long-term records. Our results suggest that conditions non-analogue to the 20th and 21st Centuries were experienced in the pre-instrumental study period and that cross-basin low flows may have increased in the past century.

2 | DATA AND METHODS

2.1 | Instrumental data and streamflow separation

Daily streamflow data from the U.S. Geological Survey (USGS) were acquired for three gages along the Arkansas River (Table 1; Figure 1): Cañon City, CO (CNC); Tulsa, OK (TLS); and Little Rock, AR (LRO) from the USGS National Water Information System. Peak flow occurs in May at LRO, and in June at CNC and TLS (Figure S1). The three USGS gage series have differing start and end dates but share a period of record from 1928 to 1970, with the LRO station ending in 1970 prior to the completion of the McKellen-Kerr navigation system (Keown et al., 1986). By combining USGS data at Little Rock with ongoing U.S. Army Corps of Engineers (USACE) daily instrumental flow data at this site (personal communication Brian Breaker), the common gauged period was extended to 1928–1980. This common period of 1928–1980 was used for all subsequent model calibrations, while flow records outside this common period were used for validation.

For each gage, daily baseflow separation was performed for the full length of record using the HYSEP sliding interval method (Sloto & Crouse, 1996), one of several common methods (Lott & Stewart, 2016). This baseflow separation approach used in the context of tree ring-based

TABLE 1 Information on flow gages used as reconstruction targets in this study

Gage	State	Abbreviation	USGS station no.	Flow variable	Month(s)	Drainage area (km^2)
Cañon City	CO	CNC-6-S	07096000	Stream	June	8073
Tulsa	OK	TLS-5-B	07164500	Base	May	192,580
Little Rock	AR	LRO-67-S	07263500	Stream	June–July	409,218
Little Rock	AR	LRO-9-B	07263500	Base	September	409,218

Abbreviation: USGS, United States Geological Survey.

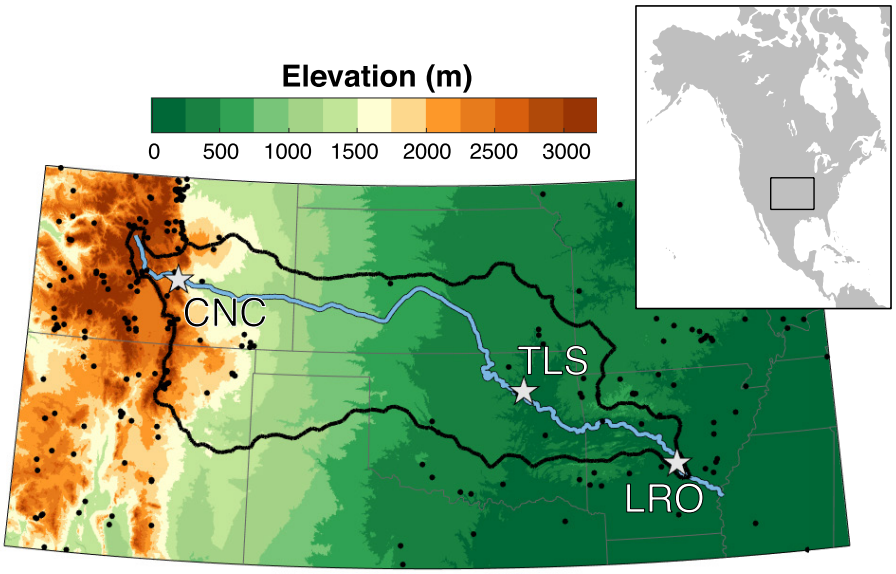

FIGURE 1 Location of the Arkansas River basin and the three instrumental gages, CNC (Cañon City, Colorado), TLS (Tulsa, Oklahoma), and LRO (Little Rock, Arkansas), used in this study. Black markers indicate available tree-ring chronologies.

reconstructions has been shown to be effective (Torbenson & Stagge, 2021) at separating slower reacting soil moisture tied to tree growth from fast surface runoff. The HYSEP method estimates baseflow based on the minimum flow for any given day (centered), with an interval that is twice the length of an assumed window (N) of surface runoff influence after a storm event (Pettyjohn & Henning, 1979). Here, $N = 0.83 \times A^{0.2}$ where A is the drainage area in square kilometers, resulting in windows of 5, 9, and 11 days for the CNC, TLS, and LRO gauges, respectively. The resulting time series were aggregated to produce a series of mean monthly baseflow and stormflow (total flow minus baseflow). Monthly and bi-monthly flow series were correlated with gridded monthly precipitation from the Climate Research Unit (CRUTS3.14; Harris et al., 2014) for a common period (1928–1980) to assess the spatial imprint and seasonal window of hydroclimatic influence on flow. While river regulation effects on baseflow estimations may vary greatly (Kolton, 1995) and are typically site-specific (Sloto & Crouse, 1996; White & Sloto, 1990), potential effects are likely minimized with greater window sizes and temporal averaging, that is, monthly baseflow estimates (Miller et al., 2015).

2.2 | Tree-ring data and predictor screening

At each of the three target gages, all available tree-ring chronologies from within a 250- (CNC, which has a higher number of nearby chronologies and more complex topography) and 500-km (TLS and LRO) radius were screened for significant correlations with baseflow and streamflow at monthly and bi-monthly intervals for a common period of 1928–1980. The 1980 end date was chosen because of the collection date of many of the available chronologies. In addition to publicly available tree-ring data from the International Tree-Ring Data Bank (Zhao et al., 2019), post oak (*Quercus stellata*) collections from Oklahoma and Texas were remeasured for earlywood (EW) and latewood (LW) widths. Tree-ring chronologies from a total of 170 sites (20 containing EW and LW measurements in addition to total-ring width) were screened against baseflow and streamflow at the three gages. Any chronology that displayed a Spearman correlation >0.405 ($p < 0.005$) with a given monthly or bi-monthly flow variable was considered a potential predictor.

Four monthly/bi-monthly flow variables were identified as reconstruction targets based on the highest correlations with the tree-ring dataset: June streamflow at Canon City (CNC-6-S); May baseflow at Tulsa (TLS-5-B); June–July streamflow at Little Rock (LRO-67-S); and

September baseflow at Little Rock (LRO-9-B). This naming scheme is used here and throughout this paper represents "Gage-Month(s)-**B**aseflow/**S**treamflow." The final predictor sets for the two downstream/eastern gages (TLS and LRO) were produced using additional screening requirements. Due to overlapping search radii, some tree-ring chronologies display significant correlations with multiple reconstruction targets. To limit the impact of shared non-hydrological variability from overlapping predictors, chronologies were only considered for the westernmost (more upstream) gage and the earliest seasonal window. For example, if a chronology was significantly correlated with May baseflow at Tulsa, it would not be considered for either of the Little Rock reconstructions. Likewise, if a chronology was chosen as a predictor for June–July streamflow at Little Rock it would not be considered for the September baseflow reconstruction. Similarly, only one type of variable (i.e., total-ring width, earlywood, latewood) would be considered at each site chronology. This series of rules is guided by the assumption that earlier seasons and upstream locations will produce a signal hydrologically closer to the soil moisture driver recorded in the local tree-ring proxy, thereby maximizing signal strength, and minimizing noise related to uncorrelated upstream flows, temporal autocorrelation in soil moisture storage, and lag/attenuation effects from surface hydrologic routing. This rule is thereby assumed to be conservative, minimizing shared variance and the likelihood of spurious downstream correlations.

2.3 | Model calibration

A principal components analysis was performed on the predictor set of tree-ring chronologies for each of the four reconstruction targets. The first principal component (PC1) was entered into a generalized linear regression model for the period 1928–1980:

$$g\left(\log\left(\hat{Q}_{\text{flow},i}\right)\right) = \beta_0 + \beta_1 \, \text{PC}_{1,i}, \tag{1}$$

where $\hat{Q}$ represents the estimated flow variable (baseflow or streamflow), for each year represented using subscript *i*. This generalized linear model assumes flows are lognormally distributed, which was verified using distribution plots.

Due to differing start dates of individual predictor chronologies, nested calibration models were produced (using the maximum number of available chronologies for any given year of reconstruction). The subsequent time series were spliced together with the shortest available nest (and therefore the most possible predictor chronologies) representing any given year in the final reconstructions. As a result, the calibration skill and associated uncertainty vary depending on what year in the reconstruction is considered, and the differing number of underlying chronologies used for calibration.

2.4 | Validation

Validation of the reconstructions was performed with several different approaches. To assess signal robustness, calibration models for the shortest nests (i.e., with the greatest number of chronologies) were also produced for split equal-length subperiods (1928–1954 and 1955–1980) at each gage, using the same predictor set as for the full period calibration (1928–1980). The alternate period was used for verification to assess the temporal stability of reconstruction skill. For gages that have observations prior to 1928, reconstructions were also compared with these instrumental data.

All pre-instrumental estimates of flow presented below are of the full calibration period (1928–1980). These reconstructions of flow were also correlated with gridded precipitation for the same seasonal windows identified as the lead hydroclimatic drivers of observed flow. Observed and reconstructed correlations and associated spatial imprints for the common period (1928–1980) and pre-calibration reconstructed data (1902–1927) were compared to confirm the flow reconstructions are capturing a historically appropriate footprint of the precipitation driver. The correlations between flow at the three gages were then compared for instrumental and reconstructed data and assessed for any bias in persistence between time series, and Fisher's *Z*-transformation was used to test the significance of differences between correlations (Fisher, 1921). In addition, qualitative comparisons with historical documentation of flow variability across the basin were performed for years of reconstructed extremes (e.g., 1826).

3 | RESULTS

The windows of strongest correlations between target instrumental flow and gridded precipitation are presented in Figure 2. June streamflow at Cañon City (CNC-6-S; Figure 2a) is driven by the preceding winter and spring precipitation (prior October–June) over the Four Corners region, reaching maximum *r*-values just west of the gage in Colorado. May baseflow at Tulsa (TLS-5-B; Figure 2b), and June–July streamflow at Little Rock (LRO-67-S; Figure 2c), are also correlated with cool-to-warm season precipitation drivers (November–May and December–July,

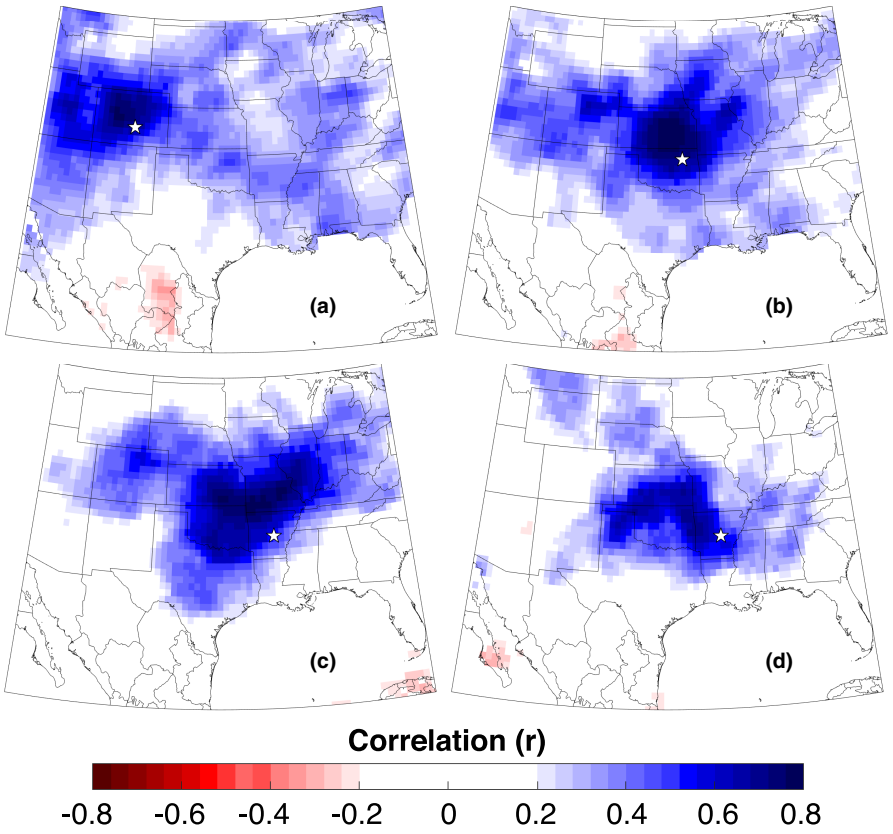

FIGURE 2 Gridded correlations between precipitation and instrumental Arkansas River flow for: (a) CNC June streamflow and October–June precipitation; (b) TLS May baseflow and November–May precipitation; (c) LRO June–July streamflow and December–July precipitation; and (d) LRO September baseflow and July–September precipitation, for the period 1928–1980. Stars represent the location of the respective gage.

respectively) for weather front patterns extending from northern Texas northeast to the Ohio River valley. September baseflow at Little Rock (LRO-9-B; Figure 2d), the lowest and latest flow from a hydrologic standpoint, displays its strongest relationship with late summer precipitation (July–September) and significant correlations are confined to the immediate surroundings of the river path upstream, suggesting a shorter and more localized response. In each case, the regions of highest correlation between precipitation and observed instrumental flow approximate a composite of the contributing upstream watershed area with the prevailing regional precipitation patterns. Each gauge's precipitation footprint is distinct enough to warrant separate reconstructions without controlling for temporal autocorrelation; note the tight clusters of high correlation immediately upstream and low correlation (white spaces) in headwater catchments for lower gauges (Figure 2c,d).

3.1 | Tree-ring predictor selection

In total, 78 tree-ring chronologies passed screening to be considered predictors. The set of predictor chronologies include a range of different species and variables (Table S1). Total-ring width records of Douglas fir (*Pseudotsuga mensiezii*), Ponderosa pine (*Pinus ponderosa*), and Engelmann spruce (*Picea engelmannii*) dominate the predictor pool at the Colorado CNC gage (total $n = 36$). At Tulsa (TLS-5-B; $n = 9$) and for the Little Rock June–July streamflow model (LRO-67-S; $n = 26$), post oak and bald cypress (*Taxodium distichum*) are the most common species. For September baseflow at Little Rock (LRO-9-B) only six chronologies make up the predictor set, all of which are shortleaf pine (*Pinus echinata*) latewood width records. Correlations between target flow and individual predictor chronologies range, depending on calibration nest, at CNC-6-S ($r = 0.410–0.536$; mean = 0.462); TLS-5-B ($r = 0.407–0.556$; mean = 0.467); LRO-67-S ($r = 0.411–0.657$; mean = 0.518); and LRO-9-B ($r = 0.417–0.727$; mean = 0.510). CNC and TLS do not have overlapping search radii due to the distance between the two gages. Eight of the nine chronologies chosen for TLS were also significantly correlated with the LRO-67-S target but were withheld from the LRO-67-S reconstruction due to selection rules outlined in the Methods. No chronologies were withheld from the LRO-9-B reconstruction because each was unique to this late-season baseflow reconstruction.

3.2 | Model calibration and validation

The four reconstructions explain shifting amounts of variance in the target flow variables, ranging from 35.8% at Tulsa (TLS-5-B) to 69.5% of June–July streamflow at Little Rock (LRO-67-S) (Figure 3). The calibration reduction of error (CRE) statistic suggests that all reconstructions are skillful in estimating past flow (Table 2). The split-period models indicate a relatively stable signal for three of the four reconstructions, with positive verification coefficient of error (CE) and verification reduction of error (RE) for both periods. The exception is LRO-9-B, for which the early calibration model (1928–1954) does not display positive verification CE and RE during the later period (1955–1980). However, the full calibration model explains over 57.8% of the variance in September flow and captures years of both extreme high and low flows (Figure 3g). Because the chronologies were screened for the full period of overlap (1928–1980), the split calibration (Table 2) cannot be considered fully independent verification but rather a test of signal stability. Overall, the predictors appear stable for both subperiods with the exception for the early calibration of LRO-9-B, which fails to produce positive verification CE and RE.

The reconstructions span varying periods of time due to differing lengths of predictor tree-ring chronologies. Reconstruction estimates for 1600–1980, with associated explained variance and number of predictors, are presented in Figure 4. The longest nests start in 837 A.D. (CNC-6-S), 998 (TLS-5-B), 997 (LRO-67-S), and 1581 (LRO-9-B), but it is worth noting that most of the early estimates are significantly less skillful. The TLS-5-B and LRO-9-B reconstructions drop below 30% explained variance prior to 1650 and the associated errors increase accordingly.

Comparing the reconstructions to gridded precipitation data for the calibration period produces correlation maps (Figure 5) that are highly similar to those based on the instrumental data. Although the spatial patterns differ (e.g., CNC-6-S has a more spatially extensive and significant imprint over the Rocky Mountains, Figure 5a than the instrumental, Figure 2a) and there are some differences in magnitude of

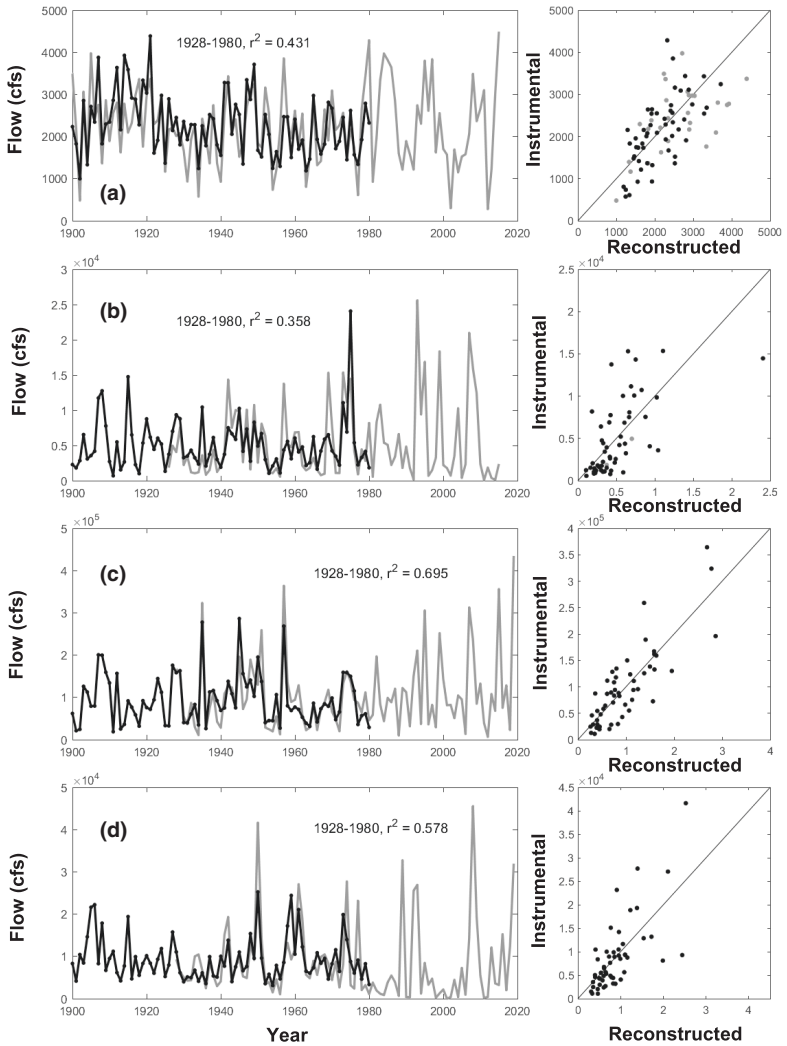

FIGURE 3 Instrumental (gray) and reconstructed (black) (a) June streamflow at CNC; (b) May baseflow at TLS; (c) June–July streamflow at LRO; and (d) September baseflow at LRO. The scatterplots (right) show calibration residuals (black) and pre-calibration residuals (gray).

TABLE 2 Statistics of reconstructions presented (CRE = calibration reduction of error)

	Calibration		Verification		
	r^2	CRE	r^2	CE	RE
CNC-6-S					
1928–1980	0.431	0.431	/	/	/
1955–1980	0.562	0.479	0.442	0.044	0.083
1928–1954	0.431	0.489	0.569	0.141	0.173
TLS-5-B					
1928–1980	0.358	0.358	/	/	/
1955–1980	0.332	0.332	0.362	0.407	0.428
1928–1954	0.453	0.387	0.471	0.276	0.277
LRO-67-S					
1928–1980	0.695	0.686	/	/	/
1955–1980	0.747	0.747	0.668	0.634	0.643
1928–1954	0.646	0.683	0.776	0.683	0.692
LRO-9-B					
1928–1980	0.578	0.192	/	/	/
1955–1980	0.163	0.271	0.478	0.169	0.169
1928–1954	0.759	0.459	0.074	−0.015	−0.015

Abbreviations: CE, coefficient of error; RE, reduction of error.

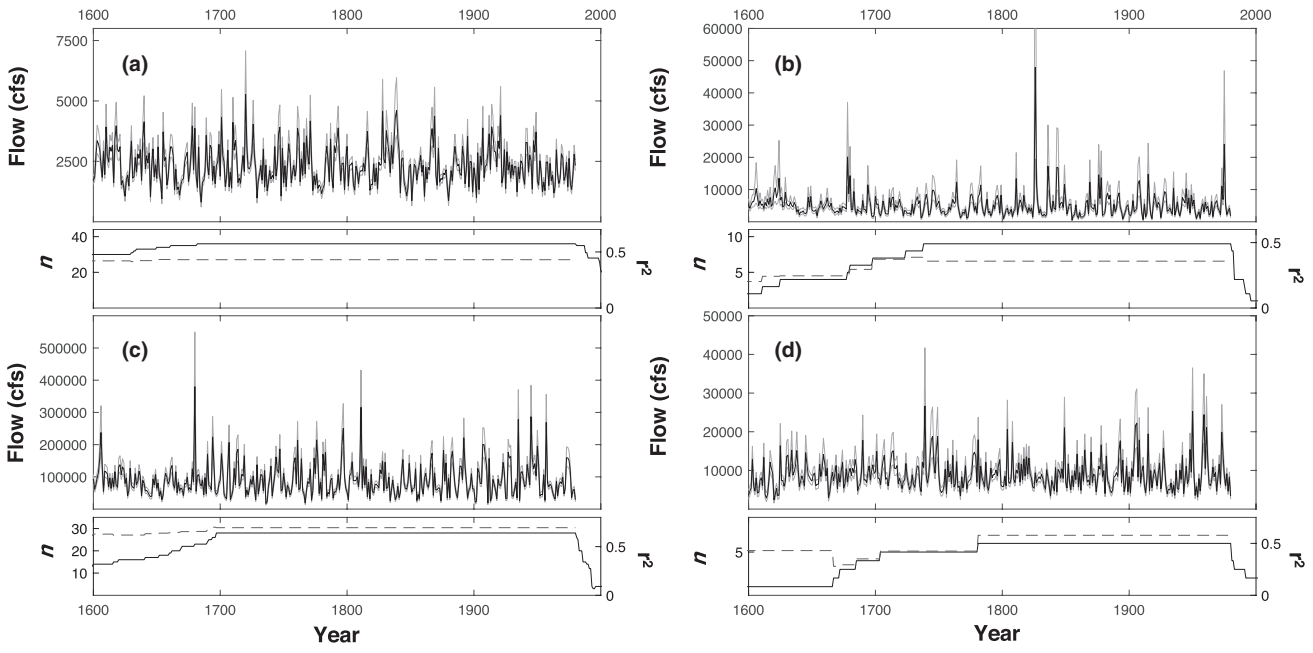

FIGURE 4 Reconstruction of Arkansas River for (a) June streamflow at CNC; (b) May baseflow at TLS; (c) June–July streamflow at LRO; and (d) September baseflow at LRO. The lower panels display the number of predictors in black, and the gray line indicates the variance explained by the different nests of each reconstruction.

correlation, the overall agreement is evident. Furthermore, the 1902–1927 pre-calibration estimates display similar patterns and magnitudes (Figure 5b,d,f,h). These results can be considered independent verification of the reconstruction estimates without calibration and support the notion that the reconstructions provide robust information on base- and streamflow prior to the 20th Century for selected seasonal windows.

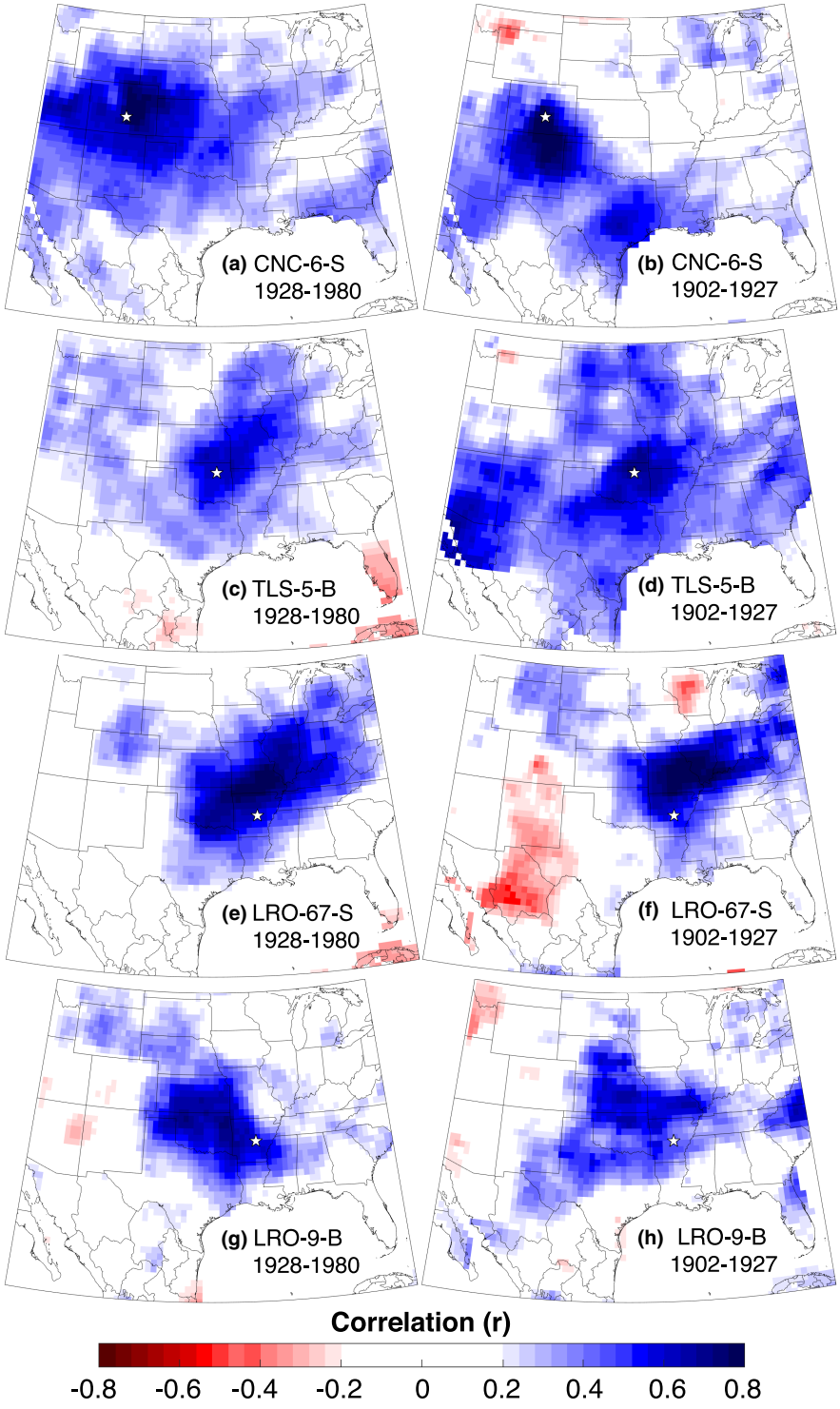

FIGURE 5 As for Figure 2 but for reconstructed flow, for the 1928–1980 calibration period (a, c, e, g), and the 1902–1927 verification period (b, d, f, h).

The approach of not allowing chronologies to be predictors at multiple sites was taken to limit non-climatic overlap of shared variance between the reconstructions. The relationships between target instrumental flows are similar to those of the reconstructions (Table 3), and no difference is statistically significant ($p > 0.05$). Maps of precipitation correlations indicate that the respective reconstructions are mainly recording the local hydroclimatic drivers of flow at the selected seasonal window. As such, we are confident that the reconstructions, and the basin-wide variability in flow, do not contain exaggerated spatial relationships and/or bias.

TABLE 3 Correlation matrix of reconstructed flow for the calibration period, 1928–1980. The same inter-gage correlations for the instrumental data are given in parenthesis. No statistically significant differences were observed between instrumental and reconstructed correlations

	CNC-6-S	TLS-5-B	LRO-67-S	LRO-9-B
CNC-6-S	X			
TLS-5-B	0.375 (0.414)	X		
LRO-67-S	0.242 (0.362)	0.566 (0.520)	X	
LRO-9-B	0.021 (−0.067)	0.164 (0.117)	0.290 (0.299)	X

4 | DISCUSSION

The Arkansas River flows through diverse landscapes and ecotones, and the predictor sets for the four reconstructions reflect a wide range of bioclimatic relationships. In the mountains of Colorado, cool season precipitation contributes to the snow cover regardless of precipitation intensity (i.e., theoretical storm vs. baseflow). Months later, snowmelt causes peak flows at Cañon City during the month of June (the month of reconstruction) and the same meltwater accessible to local trees is a limiting factor of their growth (e.g., Woodhouse, 2003). This flow generating mechanism that depends on snowmelt provides theoretical support for why total streamflow rather than baseflow in June is captured at this site.

May flow at Tulsa is largely driven by early spring rainfall over the southern Great Plains (Figure 2b). Intense rainfall events are less beneficial to many of the tree species growing in Oklahoma and northern Texas, likely due to both tree physiology and inundated surface runoff not infiltrating into the soil column for which trees access the water (Stahle & Cleaveland, 1988). As a result, the post oak chronologies from this region display higher correlations with baseflow than with streamflow and the number of potential predictors (based on significant correlations) are also greater for baseflow. The precipitation window closest related to June–July streamflow at Little Rock spans late winter to midsummer, likely connected to the less pronounced seasonality of precipitation in comparison to flow upstream. Tree-ring chronologies chosen as predictors for LRO-67-S include several records used previously in reconstructions of summer PDSI, most notably in the North American Drought Atlas (Cook et al., 1999). Conversely, September baseflow and the short window of precipitation influence (Figure 2d) limit the predictors to only short leaf pine latewood chronologies, which have an exceptional summer hydroclimate signal (Schulman, 1942; Torbenson & Stahle, 2018). The limited verification statistics for the more recent period (Table 2) may be attributed to the changes in instrumental data and increased human influence on flow since 1950. The conservative approach in testing the proxy records against both flow and extra-local precipitation variability guards against influences of teleconnection-like forcings, e.g., the El Niño Southern Oscillation (ENSO), that may not have been stable throughout the study period (e.g., Torbenson et al., 2019).

Ultimately, the information gained from proxies is limited by the signal recorded in the trees. The separation of streamflow into its baseflow and stormflow components can improve the strength of signal in some tree-ring chronologies, as exemplified by the TLS-5-B and LRO-9-B reconstruction and other watersheds (Torbenson & Stagge, 2021), but this is not the case for all chronologies and stream gages. For CNC-6-S and LRO-67-S, streamflow is recorded equally/stronger than baseflow, likely to be explained by both the seasonality of regional hydroclimate (and subsequent impact on the hydrological cycle) and species-specific responses to soil moisture.

4.1 | Persistence in flow across space and time

All four reconstructions display significant skill in estimating instrumental flow, or components of flow, for the calibration period (Table 2). Correlations between the tree-ring based estimates of flow with seasonal gridded precipitation (the season most closely tuned to respective flow during the calibration period) suggest stable relationships for pre-calibration years (Figure 5). However, because the Arkansas River has an underlying watershed structure linking upstream to downstream sites with nested catchment areas, a full evaluation of the four reconstructions must also consider correlations between stations in addition to the predictors-target perspective. Because the flow signal recorded by the trees is driven by local precipitation, it is assumed that correlations between reconstructions at selected seasonal windows would be lower than for the instrumental data, which also incorporates upstream precipitation influence. If correlations between individual reconstructions are higher than for their instrumental counterparts, it is possible that biological persistence has introduced bias to the basin-wide perspective.

As shown by the correlations between the reconstructed time series of flow (Table 3), reconstructed pairings display similar, and in some cases lower, magnitudes of correlation to the instrumental data. An example of how the localized signal in the tree-ring record differs from the instrumental data is evident for the LRO-67-S reconstruction. While the correlation between the reconstruction and precipitation is limited to the region surrounding the stream gage (Figure 5e,f), the instrumental flow record at Little Rock also displays significant correlations with precipitation variability upstream over the river's headwaters in Colorado (Figure 2c). The only correlation in the reconstructions for pairings with

$r > 0.3$ is recorded for TLS-5-B and LRO-67-S (Table 3), and even here the difference is non-significant. Nonetheless, the predictor chronologies used for LRO-67-S undoubtedly contain some late spring precipitation signal and the carryover into the June–July reconstruction is to a certain degree unavoidable. However, residual analysis suggests that there is some skill, albeit modest, in the independent time series (i.e., TLS-5-B minus LRO-67-S) for downstream flow prediction.

Furthermore, a general agreement exists between the co-occurrence of low (<25th percentile) and high (>75th percentile) flow in the instrumental and reconstructed data for the 20th Century, as measured by the number of gages (of the four considered) beyond these low/high thresholds (Figure 6). The reconstructions mimic the decadal-to-subdecadal shifts in basin-wide conditions from the 1940s (high flows) to the early 1950s (low), and the years around 1960 (high). The co-occurrences of high flows in the mid-1970s (including 1973) are also faithfully recorded by the reconstructions. Therefore, we argue that the co-occurrence of low/high flow in two or more reconstructions is indicative of inter-basin/multi-season extremes. Co-occurring low and/or high flows (and opposite sign extremes) for the pre-calibration and calibration periods are presented in Figure 7.

4.2 | Pre-instrumental examples of co-occurring extremes

The four reconstructions of Arkansas River flow span differing lengths of time but are all well-replicated from 1600 onwards. The most extreme low and high flows for 1600–1980 are recorded prior to the 20th Century for all four estimates (Table 4). Although flow at Cañon City has been measured since the late 19th Century, measurements in the eastern part of the basin do not start until the late 1920s. The agreement between eastern reconstructions (TLS-5-B, LRO-67-S, and LRO-9-B) and gridded precipitation data prior to the calibration period is an important validation of the skill of past estimates (Figure 5). Historical records provide further verification of the reconstructions, including years of extreme flow.

Despite targeting somewhat different seasons, the CNC-6-S estimates are highly correlated ($r = 0.799$ for 1600–1980) with the Woodhouse et al. (2011) reconstruction, which provides a longer and more detailed account of pre-instrumental extremes. The similarity between the two reconstructions is likely due to an overlapping pool of tree-ring chronology predictors. Among years that stand out near the headwaters is the low flow of 1851, a year previously highlighted as an exceptional drought along the front range of the Colorado Rocky Mountains (Woodhouse et al., 2002).

Although there are only instrumental measurements of flow since 1928 at the two eastern gages, a wealth of historical information (including newspaper reports and personal accounts) from almost a century prior is available. Reconstructed estimates that stand out include the high flows of 1904 for TLS-5-B, a year during which Tulsa experienced spring flooding (Patton, 1989). Water volumes subsided somewhat downstream but reconstructed values for other years indicate sustained high flows at Little Rock over several months (as indicated by the LRO-67-S and LRO-9-B reconstructions; Figure 7). In 1844, estimated May baseflow at Tulsa and both June–July streamflow and September baseflow at Little Rock were all high. Historic records mention heavy flooding in the state of Arkansas along the river and that additional heavy rains fell in July (Hickmon, 1920). The nearby White River is also thought to have seen significant flooding (Meko & Therrell, 2020). Flow in Colorado was also above average in 1844, the last year before the extensive western Great Plains drought (Woodhouse et al., 2002; Figure 7). In 1836, Arkansas experienced early flooding in April (Hickmon, 1920), not picked up by LRO-67-S which reconstructs total streamflow several months

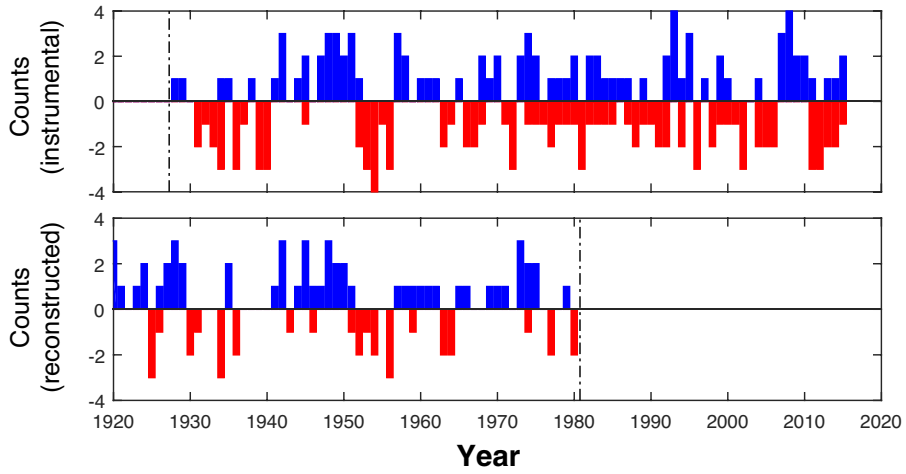

FIGURE 6 Counts of gages below and above the respective 25 (red) and 75 (blue) percentiles of flow (1928–1980) for the instrumental (top); and reconstructed (bottom) data.

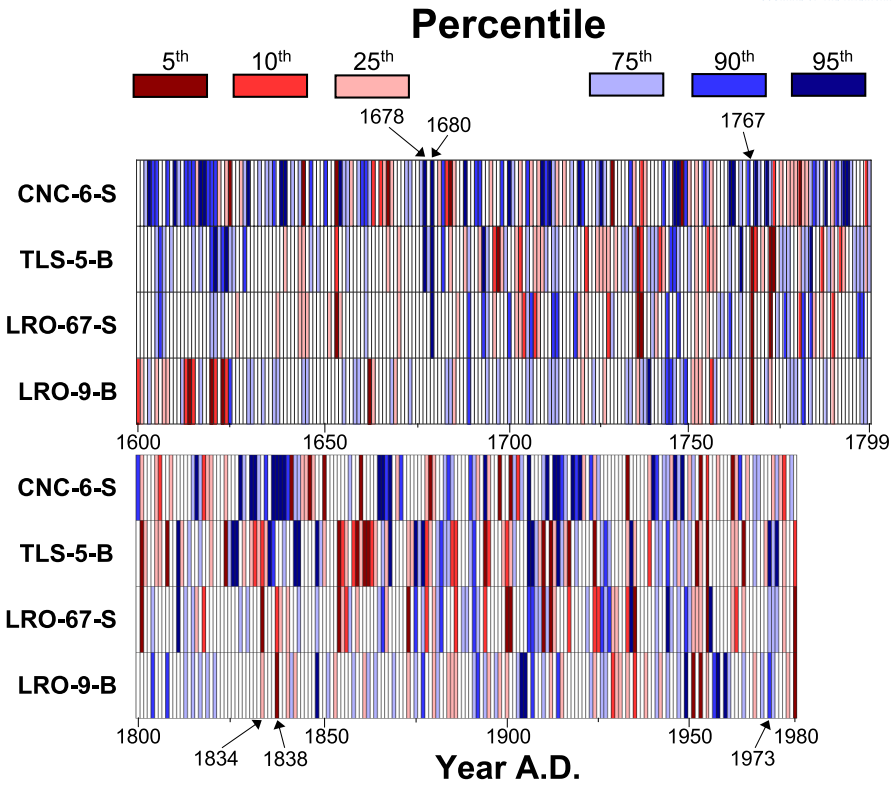

FIGURE 7 Temporal distribution of low (<5th, 10th, and 25th percentiles) and high (>75th, 90th, and 95th percentiles) flows for four reconstructions based on the 1928–1980 calibration period for respective target. Arrows indicate years mentioned in the text.

TABLE 4 The 5 years of most extreme high and low flow for respective reconstruction, 1600–1980

	CNC-6-S		TLS-5-B		LRO-67-S		LRO-9-B	
	Year	cfs	Year	cfs	Year	cfs	Year	cfs
Low	1685	812.69	1855	519.34	1736	17,513.88	1620	2393.56
	1851	869.61	1911	697.39	1911	18,929.79	1614	2861.75
	1880	883.31	1895	886.25	1767	19,236.87	1663	2977.65
	1654	954.39	1918	1006.82	1901	21,203.68	1954	3113.61
	1729	985.22	1801	1031.06	1737	23,296.49	1980	3364.35
High	1720	5268.36	1826	47,928.53	1680	379,659.61	1739	26,642.55
	1839	4610.00	1975	24,064.03	1811	315,759.88	1950	25,267.19
	1828	4569.92	1678	20,119.17	1945	286,549.65	1959	24,423.54
	1921	4389.20	1836	17,247.04	1935	277,868.20	1906	22,231.76
	1869	4371.64	1843	16,877.72	1957	268,681.27	1905	21,628.77

Abbreviation: cfs, cubic feet per second.

later in June–July. This extreme year was recorded by the TLS-5-B reconstruction, however, 1 month later and upstream, as the fourth highest May baseflow for the period 1600–1980 (Table 4). Less than two decades prior, in 1826 at Tulsa, extremely high baseflows are reconstructed, with magnitudes almost double that of the next highest flood estimate for the reconstruction period. Spring flooding on the river was documented in the historical record, causing failure of mail delivery in May and late summer (Hickmon, 1920).

Transportation was also hampered in 1834, but this time due to low flows (Hickmon, 1920), which coincides with the 6th lowest year in the June–July reconstruction for Little Rock (LRO-67-S; Figure 7). Similarly, 1829 is highlighted as an anomalous year in the historical records: the Arkansas River at Little Rock was not navigable due to scarce precipitation (Hickmon, 1920). The LRO-67-S estimate for 1829 is less than 65% of the long-term mean. Other notable years of low flow include 1838 (LRO-67-S and LRO-9-B; Figure 7) and 1839 (LRO-67-S), which may have been among the driest years of the central U.S. in recent centuries and may have exacerbated the devastation during the Trail of Tears (Perdue & Green, 2007; Torbenson & Stahle, 2018).

Prior to the 19th Century and the presence of historical records, there are several years of note that may provide scenarios of hydrologic variability that fall outside the range of the instrumental period. Similar conditions to the 1834 and 1838 low flows in the eastern part of the basin, and possibly more extreme, are indicated by the reconstructions for 1767 (Figure 7). Stretches of extended low/high flows are also recorded. For example, TLS-5-B estimates 7 years between 1800–1900 with higher flows than 1908—a year of devastating flooding in Tulsa (Patton, 1989), for which TLS-5-B records higher flows than all but one of the reconstructed values during the calibration period (1928–1980). No such high flows occurred during the 18th Century. The 18th Century did see many extended periods of low flow, however, including consecutive years of flow below the calibration mean during the periods 1720–1728 and 1751–1759 (the latter overlapping with extended low flows in the upper Missouri River; Frederick & Woodhouse, 2020). Conversely, the low late summer baseflow experienced in Little Rock over the past 40 years (post-calibration, Figure 3d) have no equivalent in the 1600–1980 reconstruction period (with the possible exception of a decade around 1615, which in part occurred during above-mean flows for June–July and Tulsa May baseflow; Figure 7). This may be a bias of the relatively short calibration period that does not contain as extreme low flows or variability in river regulation among pre- and post-calibration periods.

4.3 | Arkansas River contributions to LMRV flooding

The importance of Arkansas River flow variability on downstream flood risk is well documented (e.g., Keown et al., 1986). The flooding of New Orleans in 1973 coincided with high flows on the entirety of the Arkansas (Figure 7), undoubtedly a compounding factor in combination with high flows from the Upper Mississippi River Valley. Perhaps, the most relevant of the four reconstructions is LRO-67-S, which is closest to the confluence of the Arkansas-Mississippi rivers and also represents the stream gage having the season of highest flows. The 'Great Mississippi Flood' of 1927 falls just outside of the 1928–1980 calibration period (Barry, 2007) and ranks in the 95th percentile of reconstructed LRO-67-S flow. Flows of similar magnitude are estimated for 1908—a year during which waters were above the flood stage for over 100 days at the confluence of the Arkansas-Mississippi rivers (Hoyt & Langbein, 1955). Prior to the 20th Century, high flows are estimated for several known flood years on the lower Mississippi. The June–July streamflow reconstruction at Little Rock indicates three consecutive years of extreme flow in 1882 (>90th percentile), 1883 (>95th percentile), and 1884 (>80th percentile)—1882 and 1883 saw extensive flooding in the LMRV (Hoyt & Langbein, 1955; O'Brien, 2002).

The reconstructions presented here can inform on the relative contributions of Arkansas River flow to flood conditions in the LMRV, and by deduction, may also indicate when documented LMRV floods were driven by high flows from the Missouri and/or the Ohio Rivers when high flows are absent in the Arkansas River. The Arkansas River typically contributes 15%–20% of the annual Mississippi River peak flow measured at Vicksburg, MS (USGS gage 07289000), though extreme years may increase this proportion to 30%–40%. Major New Orleans flooding in 1851 coincides with low Arkansas River flows, suggesting that flooding originated elsewhere in the larger watershed. Among early 19th Century floods in New Orleans, 1816 and 1828 stand out (Colten, 2000). In 1828, high waters on the Arkansas River are recorded in LRO-67-S and these high flows are likely to have contributed to the record-breaking flood in New Orleans. During 1816, however, the Arkansas River was low (~10th percentile) and the month-long flooding of the Mississippi was likely caused by above-mean flows from the Upper Mississippi River Valley.

Paleoclimate studies have indicated that the flood frequency of the Lower Mississippi River has increased due to human engineering (Munoz et al., 2018). It has also been suggested that ENSO plays a role in the frequency and magnitude of flooding (e.g., Munoz & Dee, 2017). Because the most robust and stable impact of ENSO on precipitation is recorded in the U.S. Southwest, it is plausible that some of the ENSO signal in the LMRV flooding stems from Arkansas River input. This hypothesis is further supported by ENSO's reversed precipitation signal over the Ohio River basin (e.g., Torbenson et al., 2019), which is one of the largest tributaries to the Mississippi River by volume. Combining information from reconstructions of individual tributary flows may offer additional information about these processes and how inter-basin agreement/disagreement can produce scenarios of low and/or high flow for the Lower Mississippi.

Previous studies have produced flow reconstructions of the Missouri (e.g., Frederick & Woodhouse, 2020; Ravindranath et al., 2019) and White rivers (Cleaveland, 2000; Cleaveland & Stahle, 1989; Meko & Therrell, 2020), and flood event chronologies based on anatomical anomalies in annual rings exist for the White (Meko & Therrell, 2020) and lower Mississippi Rivers (Therrell & Bialecki, 2015). Although there is some spatial overlap of precipitation influence for the Arkansas and White rivers, our reconstructions display independent variance similar to the instrumental data (LRO-67-S vs. White River-678-S, Cleaveland, 2000, $r = 0.755$; instrumental data for the same variables $r = 0.741$). Tree-ring records tuned to local hydroclimate variability have also been produced in basins of eastern tributaries (e.g., Maxwell et al., 2015). The Arkansas River reconstructions described here add to the list of high-resolution paleoclimatic information on past hydroclimatic variability for basins that drain into the Mississippi River. Future work should focus on merging this information for a more complete record of streamflow contributions from major tributaries for a long-term understanding of lower Mississippi River variability.

5 | CONCLUSIONS

The four reconstructions of base- and streamflow presented here display a strong signal of the same local and extra-local precipitation that drives flow variability at the respective flow gages. Furthermore, these spatial patterns of precipitation show good separation between each of the four seasonal reconstruction targets, allowing for unique reconstructions. Baseflow appears more closely tuned to tree growth for two of the four targets. The correlations between reconstruction pairs are not significantly different from that of the respective instrumental data, suggesting that there is no overestimation of persistence across space and/or seasonal windows or of spurious inflation of shared covariance. Low and high flows, beyond the magnitude of that which has been captured by the instrumental record, have occurred throughout the Arkansas River basin in the three centuries prior to 1900. These estimates offer additional scenarios of extreme flow at individual gages, but also co-occurring extreme flows across the watershed. Such co-occurring extremes in the reconstructions are assumed to stem solely from spatial persistence of the hydroclimatic drivers (i.e., precipitation) due to the nature of the proxies.

Arkansas River influence on flooding in the LMRV is evident in the century prior to instrumental flow data. Several of the historic floods of New Orleans align with exceptionally high estimated flows during the 19th and early 20th Centuries. Known flood years for which the Arkansas River reconstructions display low flows indicate that upstream tributaries were the main drivers of downstream inundation. This information, combined with other proxy records from the Mississippi River watershed, may shed light on long-term flood risk and subsequent water management and mitigation strategies for the future.

AUTHOR CONTRIBUTIONS

Max C. A. Torbenson: Conceptualization; formal analysis; investigation; methodology; software; validation; visualization; writing – original draft; writing – review and editing. **David W. Stahle:** Conceptualization; data curation; investigation; methodology; resources; writing – review and editing. **Ian M. Howard:** Conceptualization; investigation; validation; writing – review and editing. **Joshua M. Blackstock:** Formal analysis; resources; validation; writing – review and editing. **Malcolm K. Cleaveland:** Data curation; investigation; resources. **James H. Stagge:** Conceptualization; formal analysis; funding acquisition; investigation; methodology; resources; supervision; validation; writing – review and editing.

ACKNOWLEDGMENTS

The authors thank two anonymous reviewers for constructive comments that helped better the manuscript. The authors acknowledge the data contributions to the ITRDB by numerous researchers, in particular for this study: Connie Woodhouse; Michael Stambaugh; Richard Guyette, and Jesse Edmondson. This work was supported primarily by the funds from the National Science Foundation Paleo Perspectives on Climate Change (P2C2) Project No. 17-582. Additional computing services were provided by the Ohio Supercomputer Center.

CONFLICT OF INTEREST

The authors declare no conflict of interest.

DATA AVAILABILITY STATEMENT

All tree-ring chronologies used for the reconstructions are available through the International Tree-Ring Data Bank, hosted by the National Centers for Environmental Information (NOAA). The predictand flow data are available through the National Water Information System website, hosted by the USGS.

ORCID

Max C. A. Torbenson https://orcid.org/0000-0003-2720-2238
James H. Stagge https://orcid.org/0000-0002-3667-2904

REFERENCES

Barry, J.M. 2007. *Rising Tide: The Great Mississippi Flood of 1927 and How It Changed America*. New York, NY: Simon and Schuster.
Belt, C.B., Jr. 1975. "The 1973 Flood and Man's Constriction of the Mississippi River." *Science* 189: 681–84. https://doi.org/10.1126/science.189.4204.681.
Cleaveland, M.K. 2000. "A 963-Year Reconstruction of Summer (JJA) Streamflow in the White River, Arkansas, USA, from Tree-Rings." *The Holocene* 10: 33–41. https://doi.org/10.1191/095968300666157027.
Cleaveland, M.K., and D.W. Stahle. 1989. "Tree Ring Analysis of Surplus and Deficit Runoff in the White River, Arkansas." *Water Resources Research* 25: 1391–401. https://doi.org/10.1029/WR025i006p01391.
Colten, C.E. 2000. *Transforming New Orleans and Its Environs: Centuries of Change*. Pittsburgh, PA: University of Pittsburgh Pres.
Cook, E.R., D.M. Meko, D.W. Stahle, and M.K. Cleaveland. 1999. "Drought Reconstructions for the Continental United States." *Journal of Climate* 12(4): 1145–62. https://doi.org/10.1175/1520-0442(1999)012<1145:drftcu>2.0.co;2.

Costigan, K.H., and M.D. Daniels. 2012. "Damming the Prairie: Human Alteration of the Great Plains River Regimes." *Journal of Hydrology* 444–445: 90–99. https://doi.org/10.1016/j.jhydrol.2012.04.008.

Devineni, N., U. Lall, N. Pederson, and E.R. Cook. 2013. "A Tree-Ring Based Reconstruction of Delaware River Basin Streamflow Using Hierarchical Bayesian Regression." *Journal of Climate* 26: 4357–74. https://doi.org/10.1175/JCLI-D-11-00675.1.

Dodds, W., K. Gido, M.R. Whiles, K.M. Fritz, and W.J. Matthews. 2004. "Life on the Edge: The Ecology of Great Plains Prairie Streams." *Bioscience* 54: 205–16. https://doi.org/10.1641/0006-3568(2004)054[0205:LOTETE]2.0.CO;2.

England, J.F., Jr., J.E. Godaire, R.E. Klinger, T.R. Bauer, and P.Y. Julien. 2010. "Paleohydrologic Bounds and Extreme Flood Frequency of the Upper Arkansas River, Colorado, USA." *Geomorphology* 124: 1–16. https://doi.org/10.1016/j.geomorph.2010.07.021.

Ferrington, L.C., Jr. 1993. "Endangered Rivers: A Case History of the Arkansas River in the Central Plains." *Aquatic Conservation: Marine and Freshwater Ecosystems* 3: 305–16. https://doi.org/10.1002/aqc.3270030405.

Fisher, R.A. 1921. "On the 'Probable Error' of a Coefficient of Correlation Deduced from a Small Sample." *Metron* 1: 3–32.

Frederick, S.E., and C.A. Woodhouse. 2020. "A Multicentury Perspective on the Relative Influence of Seasonal Precipitation on Streamflow in the Missouri River Headwaters." *Water Resources Research* 56: e2019WR025756. https://doi.org/10.1029/2019WR025756.

Harris, I., P.D. Jones, T.J. Osborn, and D.H. Lister. 2014. "Updated High-Resolution Grids of Monthly Climatic Observations—The CRU TS3.10 Dataset." *International Journal of Climatology* 34: 623–42. https://doi.org/10.1002/joc.3711.

Hickmon, W.C. 1920. "Weather and Crops in Arkansas, 1819 to 1879." *Monthly Weather Review* 48: 447–51. https://doi.org/10.1175/1520-0493(1920)48<447:WACIAT>2.0.CO;2.

Horowitz, A.J. 2010. "A Quarter Century of Declining Suspended Sediment Fluxes in the Mississippi River and the Effect of the 1993 Flood." *Hydrological Processes* 24: 13–14. https://doi.org/10.1002/hyp.7425.

Hoyt, W.G., and W.B. Langbein. 1955. *Floods*. Princeton, NJ: Princeton University Press.

Keown, M.P., E.A. Dardeau, Jr., and E.M. Causey. 1986. "Historic Trends in the Sediment Flow Regime of the Mississippi River." *Water Resources Research* 22: 1555–64. https://doi.org/10.1029/WR022i011p01555.

Kolton, G.F. 1995. "Determination of Base-Flow Characteristics at Selected Streamflow-Gaging Stations on the Mad River, Ohio." Water-Resources Investigations Report 95-4037, U.S. Geological Survey, Columbus, OH.

Lewis, J.M., and A.R. Trevisan. 2019. "Peak Streamflow and Stages at Selected Streamgages on the Arkansas River in Oklahoma and Arkansas, May to June 2019." U.S. Geological Survey Open-File Report 2019-129, 10 pp. https://doi.org/10.3133/ofr20191129

Lott, D.A., and M.T. Stewart. 2016. "Base Flow Separation: A Comparison of Mnalytical and Mass Balance Methods." *Journal of Hydrology* 535: 525–33. https://doi.org/10.1016/j.jhydrol.2016.01.063.

Marston, L., M. Konar, X. Cai, and T.J. Troy. 2015. "Virtual Groundwater Transfers from Overexploited Aquifers in the United States." *Proceedings of the National Academy of Sciences of the United States of America* 112: 8561–66. https://doi.org/10.1073/pnas.1500457112.

Maxwell, J.T., G.L. Harley, and T.J. Matheus. 2015. "Dendroclimatic Reconstructions from Multiple Co-Occurring Species: A Case from an Old-Growth Deciduous Forest in Indiana, USA." *International Journal of Climatology* 35: 860–70. https://doi.org/10.1002/joc.4021.

Maxwell, R.S., G.L. Harley, J.T. Maxwell, S.A. Rayback, N. Pederson, E.R. Cook, D.J. Barclay, W. Li, and J.A. Rayburn. 2017. "An Interbasin Comparison of Tree-Ring Reconstructed Streamflow in the Eastern United States." *Hydrological Processes* 31: 2381–94. https://doi.org/10.1002/hyp.11188.

Meko, D.M., and M.D. Therrell. 2020. "A Record of Flooding on the White River, Arkansas, Derived from Tree-Ring Anatomical Variability and Vessel Width." *Physical Geography* 41: 83–98. https://doi.org/10.1080/02723646.2019.1677411.

Meko, D.M., C.A. Woodhouse, C.A. Baisan, T. Knight, J.J. Lukas, M.K. Hughes, and M.W. Salzer. 2007. "Medieval Drought in the Upper Colorado River Basin." *Geophysical Research Letters* 34. https://doi.org/10.1029/2007GL029988.

Miller, M.P., H.M. Johnson, D.D. Susong, and D.M. Wolock. 2015. "A New Approach for Continuous Estimation of Baseflow Using Discrete Water Quality Data: Method Description and Comparison with Baseflow Estimates from Two Existing Approaches." *Journal of Hydrology* 522: 203–10. https://doi.org/10.1016/j.jhydrol.2014.12.039.

Mock, C.J. 1991. "Drought and Precipitation Fluctuations in the Great Plains during the Late Nineteenth Century." *Great Plains Research* 1: 26–57.

Munoz, S.E., and S.G. Dee. 2017. "El Niño Increases the Risk of Lower Mississippi River Flooding." *Scientific Reports* 7: 1772. https://doi.org/10.1038/s41598-017-01919-6.

Munoz, S.E., L. Giosan, M.D. Therrell, J.W.F. Remo, Z. Shen, R.M. Sullivan, C. Wiman, M. O'Donnell, and J.P. Donnelly. 2018. "Climatic Control of Mississippi River Flood Hazard Amplified by River Engineering." *Nature* 556: 95–98. https://doi.org/10.1038/nature26145.

Naeser, R.B., and L.L. Bennett. 1998. "The Cost of Noncompliance: The Economic Value of Water in the Middle Arkansas River Valley." *Natural Resources Journal* 38: 445–63.

O'Brien, G. 2002. *Making the Mississippi River over Again: The Development of River Control in Mississippi*. Jackson, MS: Mississippi Historical Society.

Pant, R., K. Barker, and T.L. Landers. 2015. "Dynamics Impacts of Commodity Flow Disruptions in Inland Waterway Networks." *Computers & Industrial Engineering* 89: 137–49. https://doi.org/10.1016/j.cie.2014.11.016.

Patton, A. 1989. *Fifty Years Remembered*. Tulsa District: U.S. Army Corps of Engineers.

Perdue, T., and M.D. Green. 2007. *The Cherokee Nation and the Trail of Tears*, 189 pp. New York, NY: Penguin Publishing.

Pettyjohn, W.A., and R. Henning. 1979. *Preliminary Estimate of Ground-Water Recharge Rates, Related Streamflow and Water Quality in Ohio*. Washington, DC: U.S. Department of the Interior.

Qiao, L., C.B. Zou, C.F. Gaitán, Y. Hong, and R.A. McPherson. 2017. "Analysis of Precipitation Projections over the Climate Gradient of the Arkansas Red River Basin." *Journal Applied Meteorology and Climatology* 56: 1325–36. https://doi.org/10.1175/JAMC-D-16-0201.1.

Ravindranath, A., N. Devineni, U. Lall, E.R. Cook, G. Pederson, J. Martin, and C. Woodhouse. 2019. "Streamflow Reconstruction in the Upper Missouri River Basin Using a Novel Bayesian Network Model." *Water Resources Research* 55: 7694–716. https://doi.org/10.1029/2019WR024901.

Schulman, E. 1942. "Dendrochronology in Pines of Arkansas." *Ecology* 23: 309–18. https://doi.org/10.2307/1930670.

Sloto, R.A., and M.Y. Crouse. 1996. "HYSEP: A Computer Program for Streamflow Hydrograph Separation and Analysis." Water-Resources Investigations Report 96-4040, U.S. Geological Survey, Lemoyne, PA.

Stahle, D.W., and M.K. Cleaveland. 1988. "Texas Drought History Reconstructed and Analyzed from 1698 to 1980." *Journal of Climate* 1: 59–74. https://doi.org/10.1175/1520-0442(1988)001<0059:TDHRAA>2.0.CO;2.

Therrell, M.D., and M.B. Bialecki. 2015. "A Multi-Century Tree-Ring Record of Spring Flooding on the Mississippi River." *Journal of Hydrology* 529: 490–98. https://doi.org/10.1016/j.jhydrol.2014.11.005.

Torbenson, M.C.A., and J.H. Stagge. 2021. "Informing Seasonal Proxy-Based Flow Reconstructions Using Baseflow Separation: An Example from the Potomac River, United States." *Water Resources Research* 57: e2020WR027706. https://doi.org/10.1029/2020WR027706.

Torbenson, M.C.A., and D.W. Stahle. 2018. "The Relationship between Cool and Warm Season Moisture over the Central United States, 1685–2015." *Journal of Climate* 31: 7909–24. https://doi.org/10.1175/JCLI-D-17-0593.1.

Torbenson, M.C.A., D.W. Stahle, I.M. Howard, D.J. Burnette, J. Villanueva-Diaz, E.R. Cook, and D. Griffin. 2019. "Multidecadal Modulation of the ENSO Teleconnection to Precipitation and Tree Growth over Subtropical North America." *Paleoclimatology and Paleoceanography* 34: 886–900. https://doi.org/10.1029/2018PA003510.

USACE (United States Army Corps of Engineers). 2006. *Arkansas River Drought Contingency Plan*. Little Rock, AR: Department of the Army, Little Rock District Corps of Engineers.

White, K.E., and R.A. Sloto. 1990. "Base-Flow-Frequency Characteristics of Selected Pennsylvania Streams." Water-Resources Investigations Report 90-4160, U.S. Geological Survey, Harrisburg, PA.

Woodhouse, C.A. 2003. "A 431-yr Reconstruction of Western Colorado Snowpack from Tree Rings." *Journal of Climate* 16: 1551–61. https://doi.org/10.1175/1520-0442(2003)016<1551:AYROWC>2.0.CO;2.

Woodhouse, C.A., J.J. Lukas, and P. M. Brown. 2002. "Drought in the Western Great Plains, 1845–56." *Bulletin of the American Meteorological Society* 83: 1485–94. https://doi.org/10.1175/BAMS-83-10-1485.

Woodhouse, C.A., G.T. Pederson, and S.T. Gray. 2011. "An 1800-yr Record of Decadal-Scale Hydroclimatic Variability in the Upper Arkansas River Basin from Bristlecone Pine." *Quaternary Research* 75: 483–90. https://doi.org/10.1016/j.yqres.2010.12.007.

Zhao, S., N. Pederson, L. D'Orangeville, J. Hille Ris Lambers, E. Boose, C. Penone, B. Bauer, Y. Jiang, and R.D. Manzanedo. 2019. "The International Tree-Ring Data Bank (ITRDB) Revisited: Data Availability and Global Ecological Representativity." *Journal of Biogeography* 46: 355–68. https://doi.org/10.1111/jbi.13488.

SUPPORTING INFORMATION

Additional supporting information can be found online in the Supporting Information section at the end of this article.

How to cite this article: Torbenson, Max C. A., David W. Stahle, Ian M. Howard, Joshua M. Blackstock, Malcolm K. Cleaveland, and James H. Stagge. 2022. "Pre-instrumental Perspectives on Arkansas River Cross-watershed Flow Variability." *Journal of the American Water Resources Association* 00 (0): 1–15. https://doi.org/10.1111/1752-1688.13068.